IEEE Transactions on Nuclear Science, Vol.NS-24, No.3, June 1977

OBSERVATION AND SUPPRESSION OF RADIAL BEAM BLOWUP IN THE MARYLAND ERA*

W. W. Destler, D. W. Hudgings, and M. J. Rhee
University of Maryland
College Park, Maryland 20742

Summary

In the Maryland ERA, a rotating electron ring beam is produced by passing a nonrotating hollow beam through a narrow magnetic cusp. As the beam progresses in the acceleration region downstream of the cusp transition, a fast growth in the radial thickness of the beam is observed, resulting in rapid loss of the beam to the conducting boundaries. The effect of different conducting boundary configurations on the radial growth of the beam has been measured using magnetic probes and time-resolved and time-integrated photographs of the beam cross section. Measurements of the microwave radiation produced by the beam as it propagates in the downstream region indicate that a substantial fraction of the total beam power is converted into radiation. This radiation is attributed to the negative mass instability and coupled into the TE and TM waveguide modes of the downstream drift chamber. When the beam is passed through a 6.4 mg-cm^{-2} titanium foil located at the anode plane, microwave radiated power is reduced by a factor of 100 and the radial blowup of the beam is suppressed.

I. Introduction

The basic concept behind the electron ring accelerator involves the trapping of a number of positive ions in the potential well of a dense relativistic electron ring. As long as the number of trapped ions is only a small fraction of the number of electrons in the ring, the ion loaded ring may be accelerated to high velocity using externally applied electric or magnetic fields.

In the Maryland ERA,[1] dense, relativistic electron rings and E-layers are generated by passing a hollow, straight electron beam through a narrow magnetic cusp. In this paper, experiments are reported in which a rapid radial blowup of the beam is observed in the region downstream of the cusp transition. The radial width of the beam is observed to grow to values well in excess of those predicted by single particle calculations[2] or an equilibrium model,[3] and is accompanied by the production of intense, broadband microwave radiation. Experiments will be reported in which the blowup has been effectively suppressed by scattering the beam electrons through thin foils located upstream of the cusp transition. These results will be discussed in terms of the negative mass instability.

II. Experiments

The general experimental configuration is shown in Fig. 1. In the experiment, two opposing solenoids are used to form a magnetic cusp, and the downstream solenoid is extended to provide a drift region in which the particle motion is essentially adiabatic. The transition width of the cusp is narrowed substantially by a soft iron plate placed between the solenoids. A hollow relativistic electron beam (2.5 MeV, 30 kA) is emitted from a circular knife-edge cathode located 12 cm upstream of the cusp transition. The radius of the cathode is 6 cm. A brass plate attached to the surface of the iron plate serves as the anode. The electrons pass through an annular slit in the iron plate, and the effective area of the slit may be varied to provide some control over the total current propagating into the downstream drift region. The experiments were performed at sufficiently good vacuum (about 10^{-5} torr) to ensure that charge neutralization of the electron beam is negligible upstream and downstream of the cusp transition.

The downstream beam propagates within a cylindrical drift tube 3 meters in length and 15 cm in inner diameter. This drift tube may be either of the standard solid conducting wall configuration or a "squirrel cage" conductor designed to provide a conducting boundary without azimuthal image currents. Such conductors are designed to provide an axial focusing of the downstream beam. A "squirrel cage" inner conductor of outer radius 4.5 cm may be inserted from the downstream end of the drift tube.

<u>Measurements of the downstream beam self-magnetic field</u>. Very fast (less than 1 nanosecond risetime) integrated $\dot{B}$ loops have been used to measure the axial component of the self-magnetic field of the beam on axis at various axial positions. The self-magnetic field provides an indication of the current density J_θ in the beam, and the time of flight of the beam between two probes separated by a known axial distance provides an estimate of the beam axial velocity. This axial velocity and the pulse length of the magnetic probe signals provide an estimate of the axial length of the beam.

A simple theoretical model[4] has been constructed to aid in the interpretation of the magnetic probe data. An axial current $I_o(t)$ is assumed to pass through the cusp into the downstream drift region. No instantaneous spread in electron energy is present at the cusp plane, but an electron axial velocity v(t) is assumed at this point. Thus, at any position downstream of the cusp, the electron density may be written:

$$n(z,t) = \frac{I_o(t')/e}{\left| v(t') - \frac{dv(t')}{dt'}(t-t') \right|}$$

where $t' = t - z/v(t')$. The axial component of the self-magnetic field produced at this point is therefore

$$B_z(z,t) = \int_0^t \frac{\mu_o r_o^{\,3} \omega_c I_o(t')dt'}{2\{r_o^{\,2} + [z - v(t')(t-t')]^2\}^{3/2}} \tag{1}$$

where $\omega_c = \frac{eB_o}{m_o\gamma}$ is the relativistic electron cyclotron frequency and r_o is the beam radius. As collective effects have been ignored in this model, it will serve primarily as an indication of when beam behavior deviates from single-particle expectations. In the actual calculations, v(t) was approximated by a sine function with a half period of 3 ns.

Figure 2 shows a plot of observed and calculated [using equation (1)] magnetic probe signals at z = 25 cm in the downstream field. In these experiments, the anode plane transmission area was only 40% of the total area of the annular slit in the iron plate, and a solid outer conducting boundary was used. Good agreement between the experimental waveform for the unscattered beam and the calculated pulse shape was observed when the beam current I_o in the theoretical model is set at 3.1 kA, a figure consistent with independent measurements of the total beam current propagating downstream of the cusp under similar conditions. When the squirrel cage inner conductor is inserted under the same conditions, the peak self-magnetic field observed is 70% higher and the pulse duration is about half that observed with no inner squirrel cage present. When the beam is scattered through a 6.4 mg-cm^{-2} titanium foil located at the anode plane, the peak self-magnetic field is reduced substantially, as shown in the figure.

Measurements of the peak self-magnetic field of the downstream beam as a function of axial position have been obtained using a variety of conducting boundary configurations, and results are plotted in Fig. 3. Since the self-magnetic field of a beam of given current density is dependent upon the conducting boundary configuration used, the results have been normalized to facilitate comparison of the various cases. It is easily seen that the self-field of the beam falls off much more rapidly than predicted by (1) for all boundary conditions when no scattering foil is used, although the outer squirrel cage configuration appears to be more favorable. This loss in the beam self-field was observed to occur even more rapidly if the beam current is increased. For the beams scattered through a 6.4 mg-cm^{-2} titanium foil located at the anode plane, the peak value of the self-magnetic field measured at a given axial position is reduced. However, it is interesting to note that the relative decay of the peak beam's self-magnetic field versus distance appears to follow the single particle curve.

Time-integrated beam radial width. The cause of the loss in beam self-magnetic field observed is shown in Fig. 4. In these experiments, time-integrated photographs of the downstream beam cross section were obtained by open shutter photography of the light emitted when the beam strikes a clear acrylic beamstop, as shown in Fig. 1. These photographs were scanned radially using a densitometer and the results unfolded using the film response curve to provide an estimate of the time-integrated electron density as a function of radius. The plots in Fig. 4 clearly show the radial spreading of the beam cross section when no scattering foil is used. This spread appears to be primarily inward. When the scattering foil is used, the radial width of the beam is much narrower, a result consistent with the magnetic probe data described previously.

Time-resolved beam radial width. Measurements of the beam radial width as a function of time were made at a fixed axial position by streak photography of a 2 mm diameter filament of NE 102 plastic scintillant placed radially in the beam path. The scintillation light risetime is effectively instantaneous, but the falltime is about 3 ns limiting the overall resolution of the experiment. Typical results are shown in Fig. 5, and show clearly the dramatic improvement in the radial confinement of the beam when the 6.4 mg-cm^{-2} scattering foil is used. These results are interesting since, from a single particle viewpoint, the scattering of the beam through the foil should result in a greater beam radial width. Thus, in this regime, collective effects appear to dominate the beam behavior.

Microwave generation and suppression. The radial blowup of the downstream beam observed in these experiments was accompanied by intense bursts of microwave radiation.[5] This radiation, attributed to azimuthal bunching of the beam electrons driven by the negative mass instability, is coupled into the TE and TM waveguide modes of the downstream drift chamber. Measurements were made at X-band (7-12 GHz) and KA-band (26-40 GHz). Radiation was observed at all harmonics of the electron cyclotron frequency covered by the available bands. The total power over all frequencies was estimated at 100 MW or greater for the 40% transmission case. The observed microwave power was a strong function of beam density, as expected if the radiation is driven by any collective instability. These results are consistent with the observed loss in the mean radius of the downstream beam described previously. When the beam is scattered through the 6.4 mg-cm^{-2} titanium foil, observed radiated power in these two bands was reduced by a factor of more than 100.

III. Conclusions

A radial blowup of the hollow, rotating electron beams of the Maryland ERA experiment has been observed. This radial growth is primarily attributed to the negative mass instability and is accompanied by intense microwave radiation at harmonics of the electron cyclotron frequency. The phenomenon is strongly dependent upon beam density, as expected if the growth is driven by any collective instability. Theoretical analyses of the negative mass instability in electron rings and E-layers have concluded that the instability may be suppressed by providing a spread in the particle energy. The resultant spread in angular frequencies prevents the azimuthal bunching of the beam electrons which characterizes the instability. In the experiments, the spread in particle energy is provided by scattering the beam through thin foils located at the anode plane. The resultant energy spread and small angle scattering suppressed the radial growth of the beam and reduced observed microwave radiated power by more than two orders of magnitude. Further work is required to optimize foil thickness and beam current to produce the most attractive electron beam properties for ion acceleration. Initial beam trapping and ion-loading experiments are currently under preparation.

Acknowledgments

The authors are indebted to R. A. Meger and J. T. Cramer for assistance in experimental data acquisition and analysis.

References

1. W. W. Destler, D. W. Hudgings, H. Kim, M. Reiser, M. J. Rhee, C. D. Striffler, and G. T. Zorn, Proc. of 1977 Particle Accelerator Conf., Chicago, Ill.
2. M. J. Rhee and W. W. Destler, Phys. Fluids 17, 1574 (1974).
3. C. D. Striffler and H. Kim, Physics Technical Report 77-062, Univ. of Maryland.
4. M. J. Rhee and H. S. Uhm, MDERA Technical Note 76-007, Univ. of Maryland.
5. W. W. Destler, D. W. Hudgings, M. J. Rhee, S. Kawasaki, and V. L. Granatstein, submitted to J. Appl. Phys. for publication.

*Research supported by NSF Grant No. PHY7611178.

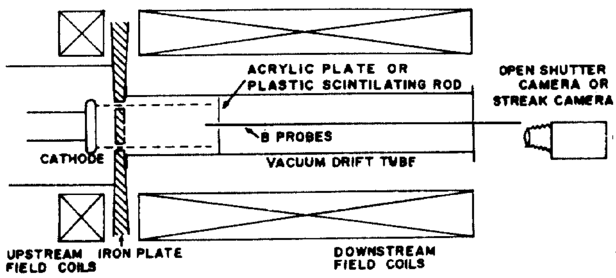

Fig. 1. Experimental configuration, with no inner conductor shown.

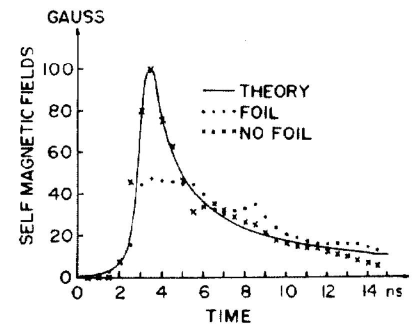

Fig. 2. Beam self-magnetic field pulses at z = 25 cm with no inner conductor.

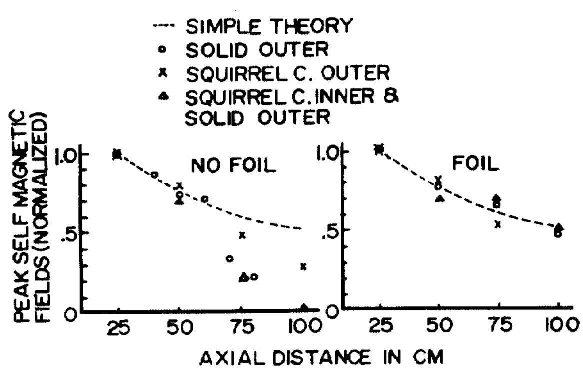

Fig. 3. Peak beam self-magnetic field, normalized to field at z = 25 cm, 40% anode.

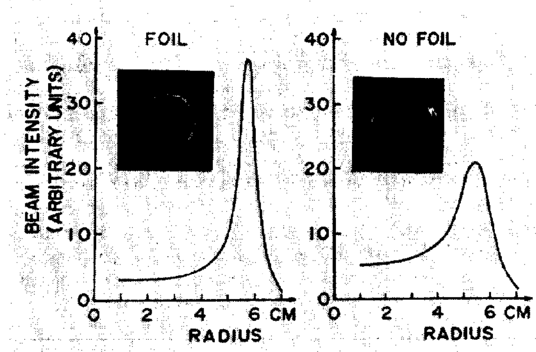

Fig. 4. Time-integrated photographs of beam cross section 1.5 meters downstream of the cusp and time-integrated beam density as determined from photographs.

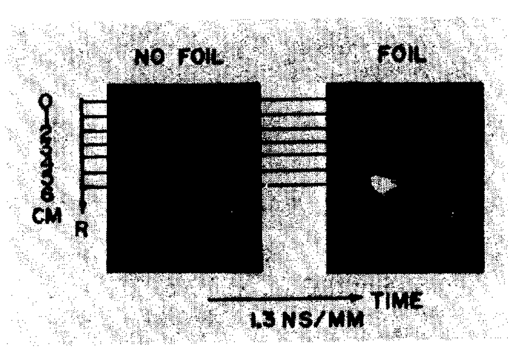

Fig. 5. Typical time-resolved beam width photographs, taken at 1.5 meters downstream of the cusp transition.